



# Micromachining using focused high energy ion beams: Deep Ion Beam Lithography

J.A. van Kan <sup>a,\*</sup>, J.L. Sanchez <sup>a</sup>, B. Xu <sup>b</sup>, T. Osipowicz <sup>a</sup>, F. Watt <sup>a</sup>

<sup>a</sup> Department of Physics, National University of Singapore, Lower Kent Ridge Road, Singapore 119260, Singapore

<sup>b</sup> Institute of Micro-Electronics, Science Park II, Singapore 117685, Singapore

---

## Abstract

The combination of deep X-ray lithography with electroforming and micromoulding (i.e., LIGA) has been shown to offer high potential for the production of high aspect-ratio microstructures. The LIGA technique, employing synchrotron light and a suitable X-ray mask, allows production of 3D microstructures in PMMA with aspect ratios around 100. Here we demonstrate that the novel technique of Deep Ion Beam Lithography (DIBL), a direct process utilizing a focused beam of MeV ions scanned in a predetermined pattern over a suitable resist material, can produce three dimensional microstructures with sub-micrometer feature sizes. Microstructures extending up to 100  $\mu\text{m}$  from the substrate with aspect ratios approaching 100 can be produced. Multiple exposures at different ion energies allow production of multilayer structures in single resist layers of SU-8, a newly developed, chemically accelerated, negative tone, near UV, photoresist. © 1999 Elsevier Science B.V. All rights reserved.

*PACS:* 07.10.Cm; 07.78.+s; 85.40.Hp

*Keywords:* Micromachining; Nuclear microscope; High aspect ratio

---

## 1. Introduction

The emerging Micro-ElectroMechanical System (MEMS) technology has high potential for the integration of microelectronics and micromechanical components. Several techniques are being developed for the production of three dimensional microstructures that can be integrated in MEMS systems. The LIGA (Lithographie, Galvano, Abformung) process is a technique currently being

used to produce 3D microstructures [1,2]. In LIGA, synchrotron X-ray radiation is passed through a mask and the transmitted X-rays are used to expose a pattern in a resist, e.g. high density PMMA. Although the technique has been used for some years now, LIGA remains expensive because of the high cost of the synchrotron accelerator. In order to develop 3D lithographies which do not require the high flux requirements of the synchrotron, new types of resist are being developed. One of these showing high potential, SU-8 [3], is a chemically amplified negative tone resist that can be used with UV light. SU-8 has been used to produce microstructures with thickness up

---

\* Corresponding author. Tel.: +65 874 2624; fax: +65 777 6126; e-mail: phyjavk@nus.edu.sg

to a few mm. Another technique to produce 3D microstructures is Stereo Lithography, a promising technique which allows the manufacture of 3D parts by a light-induced spatially resolved polymerization [4], but a limitation of this technique is the rather low accuracy [5,6].

Deep Ion Beam Lithography (DIBL) using MeV protons, is a technique which is able to produce 3D microstructures in positive resists such as PMMA as well as in negative resists such as SU-8. An advantage of DIBL is that no mask is needed to produce structures with high aspect ratios and sub-micrometer detail in the lateral direction [7,8]. In this paper two basic features of the Singapore DIBL setup will be discussed: First the implementation of a faster scanning system specifically designed for high resolution DIBL will be described. Second, the smallest feature size attainable will be shown to be determined by the lateral dose distribution of the ion beam, which varies with depth in the resist. Examples of microstructures produced with DIBL in positive resist as well as in negative resist will be shown.

## 2. Experimental procedures

The exposures presented in this paper were performed using the nuclear microscope at the Research Centre for Nuclear Microscopy of the National University of Singapore [9], where 100 nm spot sizes can be achieved for 2 MeV protons [10]. Typical currents used for micromachining range between 1 and 100 pA.

Currently we utilise magnetic scanning coils to scan the beam over a sample area. For analytical work using micro PIXE and RBS, a scanning system with a grid size of  $256 \times 256$  pixels is sufficient. For DIBL purposes however a high resolution scanning-system is essential in order to produce well defined smooth microstructures. The DIBL scanning system utilizes a Keithley ADD-16 DAC card, with a resolution of 12 bits per channel. This corresponds to a grid of up to  $4096 \times 4096$  pixels, offering increased resolution for the DIBL process [8]. During the development of the DIBL scanning system the pixel dwell time was reduced

from 300  $\mu\text{s}$  down to 50  $\mu\text{s}$  to allow more flexibility in the exposure process.

Currently the beam intensity of the HVEC AN2500 van de Graaff accelerator fluctuates rapidly, caused by the energy instability which is common in belt driven accelerators. This creates difficulties in the production of smooth microstructures. These problems will eventually be overcome when DIBL exposures are carried out with a state of the art 3.5 MV HVEC Singletron accelerator to be installed soon at the Research Centre for Nuclear Microscopy. At the present time however, in order to reduce the effect of the beam intensity fluctuation, we normalize the proton dose for each pixel in the scan pattern [8]. The insulating character of the PMMA precludes the use of the monitored beam current for normalization, so instead a large surface barrier detector is used (630 msr solid angle) to monitor backscattered nuclear collisions. Even so, this normalization is not very efficient, since full PMMA exposure occurs at only 12 backscatter events per  $\mu\text{m}^2$ . This corresponds to a dose of 100 nC/ $\text{mm}^2$ . A second method we use involves rapid scanning: An approximately even dose distribution can be obtained if many fast scans of a pattern are written, thereby averaging the beam fluctuations over each pixel exposure. This method is more suitable for sensitive resists such as SU-8 which require a much lower proton dose than the more conventional PMMA. SU-8 requires about one backscatter event per square micrometer, equivalent to about 13 nC/ $\text{mm}^2$ .

After exposure the samples are developed in a chemical solution. The type of developer depends on the resist type, and the development time depends on the thickness of the resist layer and temperature. The thick PMMA samples were developed following the procedures given in [7]. The SU-8 was developed at room temperature using SU-8 developer for 3–7 min.

## 3. Results

Figs. 1 and 2 show structures made in a thick piece (2 mm) of PMMA resist using a 2 MeV proton beam with a spot size close to 1  $\mu\text{m}^2$ . The

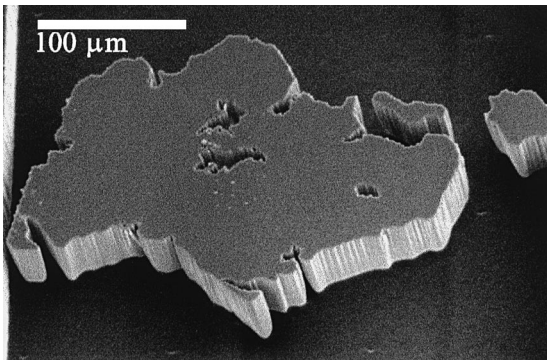


Fig. 1. SEM micrograph of a map of Singapore produced in bulk PMMA using a direct-write 2 MeV proton beam.

beam dose per pixel was controlled using nuclear backscatter normalization. Both structures were exposed in an area of  $400 \times 400 \mu\text{m}^2$  using  $512 \times 512$

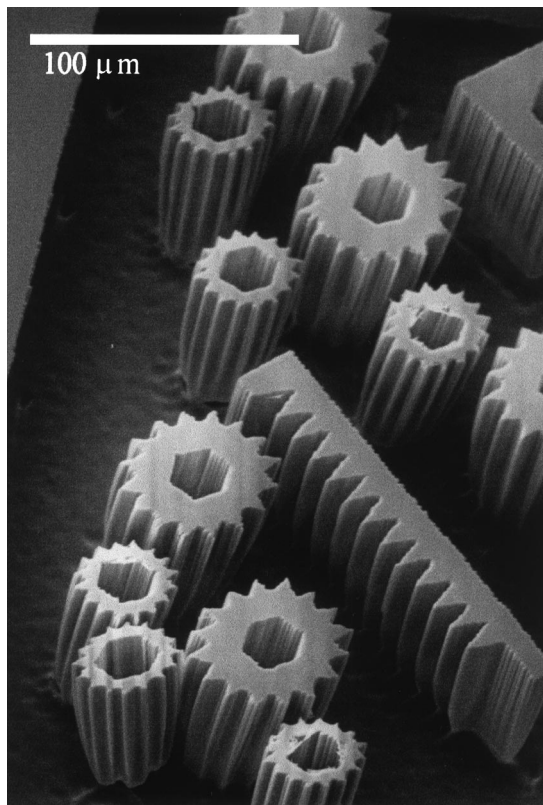


Fig. 2. SEM micrograph of cogs produced in bulk PMMA using a direct-write 2 MeV proton beam.

pixels. The structures have a height of  $63 \mu\text{m}$ , the range of 2 MeV protons in PMMA.

The direct write process does not require a mask, therefore complicated features can be produced easily. In Fig. 1 a map of Singapore is shown. In Fig. 2 cogs produced using DIBL are displayed. The bottom left cog has become detached from the bulk PMMA, probably weakened structurally by the spread of the beam at the end of range. The end of range spread, coupled with higher energy deposition, produces an undercut in the structures at the end of range. This can be seen at the bottom of all the structures in Figs. 1 and 2. The largest aspect ratio of the cogs in Fig. 2 is about 20. Although high aspect ratios are difficult to obtain in thick PMMA because of the end of range beam broadening, high aspect ratios approaching 100 can be achieved in thin resist layers or suspended cantilevered structures [8].

Fig. 3a and b show structures produced in a single layer of SU-8 resist. The resist layer was applied on a Si wafer using the spin coating technique. The thickness of the SU-8 layer was adjusted to  $20 \mu\text{m}$  to prevent the end of range broadening occurring in the resist layer. Because SU-8 is a negative resist, the structures which remain are those which have been subjected to proton exposure. To produce the structures shown in Figs. 3a and b, two exposures were performed with 0.6 and 2 MeV protons. The 0.6 MeV protons have a range of less than  $10 \mu\text{m}$  in the SU-8 layer and therefore this exposure produced the suspended walls. The supporting walls, perpendicular to the first set, were exposed with 2 MeV protons. At 2 MeV, the protons penetrate through the whole SU-8 layer and are stopped in the supporting Si wafer. The undercutting due to the end of range damage, clearly visible in Figs. 1 and 2, is not apparent in the supporting walls in Fig. 3 because the protons are stopped in the Si wafer substrate. In the supported walls the spread of the beam is much less because the 0.6 MeV proton beam travels less than  $10 \mu\text{m}$  and spreads much less compared to the 2 MeV proton beam. The alignment of the two exposures is achieved by means of a marker on the resist layer, which is mapped using PIXE or RBS signals.

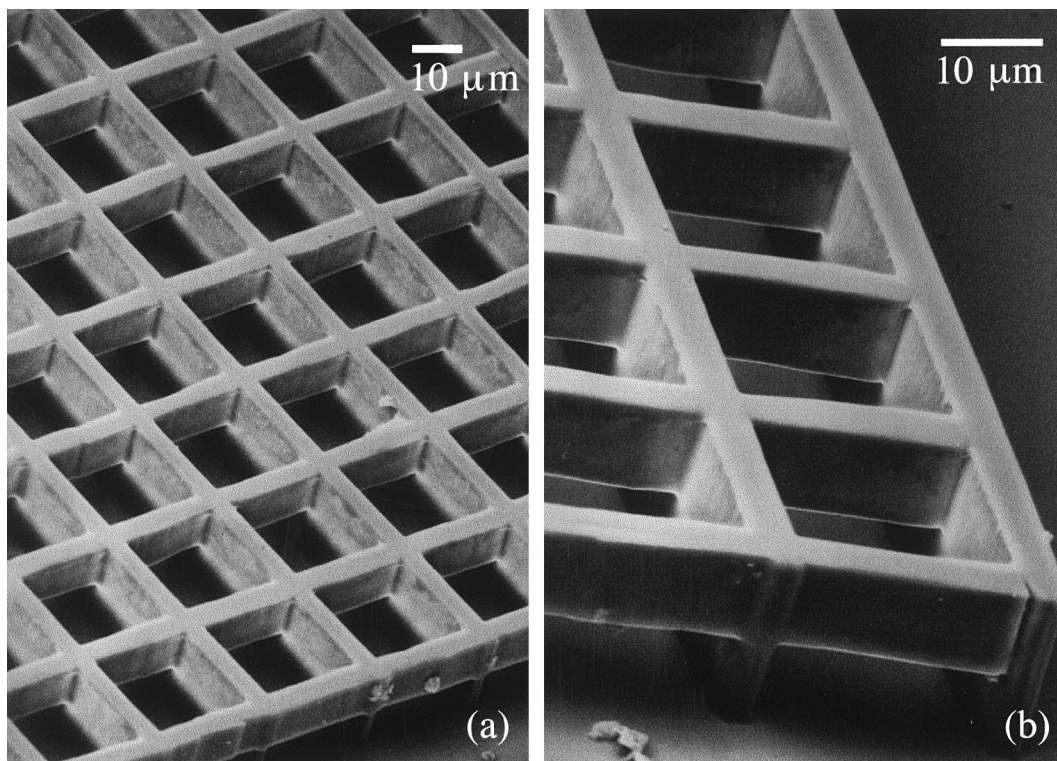


Fig. 3. Double layered grid produced in one 20  $\mu\text{m}$  layer of SU-8 resist using two exposures at proton energies of 0.6 and 2 MeV.

The spatial ionization energy distributions in carbon at two different depths were calculated for a 2 MeV proton beam. Using the Monte Carlo simulation program TRIM [11]  $10^5$  ion paths were calculated for 2 MeV protons in PMMA. The ion positions in two  $(x,y)$  planes at respective depths  $z$  of 15 and 48  $\mu\text{m}$  were convoluted with the spatial distribution of the ionization energy in carbon induced by the generated electrons as discussed in the work of Kobetich and Katz [12]. Carbon data is used for the convolution because no data for PMMA is available and 60% of the resist consists of carbon. In the calculations the  $(x,y)$  planes were divided in unit cells of  $10 \times 10 \text{ nm}^2$ . Fig. 4 shows the results of these energy deposition calculations together with the ion distributions according to TRIM. In the curves for the ion distributions it is assumed that all the energy is deposited in one unit cell ( $10 \times 10 \text{ nm}^2$ ). From Fig. 4 two effects are clear: Firstly the effect of secondary electrons on the size of the beam energy deposition is small; at a depth

of 15  $\mu\text{m}$  (Fig. 4a) the distribution has broadened slightly and at 48  $\mu\text{m}$  (Fig. 4b) there is no effect visible. Secondly, sub-micrometer features can be

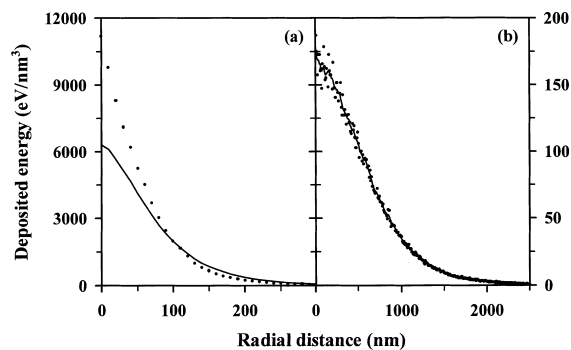


Fig. 4. Results of energy deposition calculations: Primary protons and secondary electrons: Ion distributions calculated according to TRIM for a 2 MeV proton beam at depths of (a) 15  $\mu\text{m}$  and (b) 48  $\mu\text{m}$ . The dots represent the ion energy deposition, and the lines represent the electron energy deposition.

produced in a PMMA sheet of at least 15  $\mu\text{m}$  thickness using a 2 MeV proton beam. More advanced calculations will be performed in future to determine the limit of feature sizes obtainable in DIBL.

#### 4. Conclusions

DIBL using 2 MeV protons is able to produce 3D microstructures with complex shapes and heights up to several tens of microns in positive resist such as PMMA and in negative resist such as SU-8. Preliminary Monte Carlo simulations show that sub-micrometer structures can be produced using DIBL, since the effects of the secondary electrons on the feature size is minimal; more detailed calculations are planned. Finally it is shown that DIBL is able to produce double layered complex 3D structures in the newly developed negative resist SU-8.

#### References

- [1] E.W. Becker et al., *Microelectron. Eng.* 4 (1986) 35.
- [2] W. Ehrfeld, H. Lehr, *Radiat. Phys. Chem.* 45 (1995) 349.

- [3] H. Lorenz et al., *Proceedings of MME'96, Micro Mechanics Europe, Barcelona, Spain, October 1996.*
- [4] K. Ikuta, K. Hirowatari, *Proceedings of the IEEE International Workshop on Micro Electronic Mechanical Systems*, vol. 47, 1993, p. 42.
- [5] A. Bertsch, H. Lorenz, P. Renaud, *Proceedings of MEMS IEEE, Heidelberg, Germany, 1998*, p. 18.
- [6] A. Bertsch, S. Zissi, J.Y. Jezequel, S. Corbel, J.C. Andre, *Microsystem Technologies*, vol. 47, Springer, Berlin, 1997, p. 42.
- [7] S.V. Springham, T. Osipowicz, J.L. Sanchez, L.H. Gan, F. Watt, *Nucl. Instr. and Meth. B* 130 (1997) 155.
- [8] J.L. Sanchez, J.A. van Kan, T. Osipowicz, S.V. Springham, F. Watt, *Nucl. Instr. and Meth. B* 136–138 (1998) 385.
- [9] F. Watt, I. Orlic, K.K. Loh, C.H. Sow, P. Thong, S.C. Liew, T. Osipowicz, T.F. Choo, S.M. Tang, *Nucl. Instr. and Meth. B* 85 (1994) 708.
- [10] F. Watt, T. Osipowicz, T.F. Choo, I. Orlic, S.M. Tang, *Nucl. Instr. and Meth. B* 136–138 (1998) 313.
- [11] J. Biersack, L.G. Haggmark, *Nucl. Instr. and Meth.* 174 (1980) 257.
- [12] E.J. Kobetich, R. Katz, *Phys. Rev.* 170 (2) (1968) 391.